University of Glasgow

DEPARTMENT OF

AEROSPACE ENGINEERING

The 3-D Vortex Particle Method and the Fast Summation Algorithm

L. Qian and M. Vezza

G.U. Aero Report No. 9620

The 3-D Vortex Particle Method and the Fast Summation Algorithm

L. Qian and M. Vezza

Department of Aerospace Engineering
University of Glasgow
Glasgow G12 8QQ

September 1996

The 3-D Vortex Particle Method and the Fast Summation Algorithm

L. Qian and M. Vezza

Dept of Aerospace Engineering

Abstract In this report the vortex particle method developed by G.S. Winckelmans and A. Leonard for the computation of 3-D unsteady viscous flows is briefly reviewed. Numerical results are given for the interesting phenomenon of the fusion of two vortex rings, which shows that the method works well for long time computation. To reduce the high computational cost of the direct summation, a fast hierarchical algorithm for 3-D vortex particle interactions is being implemented.

1. Introduction

The discrete vortex method is a kind of numerical method which attempts to model rotational fluid motion by discretization of the distributed(continuous) vorticity fields into finite numbers of small vortex elements. In 3-D situation, there exist two main discrete vortex methods. One is called filament methods(Leonard,1985) [1,4] in which the vortex tubes are treated as entities: they move as material volumes and they retain their circulation; i.e., they preserve their identity. But this method can only be used in inviscid flows. In viscous flows, vortex tubes do not necessarily retain their identity because of the possibility of reconnection of vortex tubes by viscous diffusion. The other is called vortex particle method or vorton method [2] which is the extended form of the 2-D point-vortex method and the vortex-blob method. This method has the advantage that the particles are somewhat independent as they do not necessarily belong to a specific vortex filament for all times and the treatment of viscous diffusion can be easily achieved. So it is more flexible and versatile than the filament method. The objecton of this method is that the vorticity field constructed by the vortex particles may not be divergence-free, which is not true in real flow problems. This problem is partly resolved by

Winckelman(1993) who developed a relaxation scheme which forces the particle vorticity field to remain nearly divergence-free.

Compared to other numerical methods (eg. finite difference or finite elements methods) the vortex method has the following merits:

(1) It is a grid-free method based on the Lagrangian principle.

(2) The computation can be limited only to the region of non-zero vorticity such as the narrow regions near the body and in the wake.

(3) The outer boundaries of the computed domain is set at infinity which removes all problems associated with computations in a truncated domain.

(4) There is low numerical dispersion and there is no CFL number.

But as other numerical methods, the discrete vortex methods also have some disadvantages :

(1) The flow has to be treated as incompressible.

(2) It is much more expensive or it has high computational cost. Since each vortex is influenced by all the others(N-body problem), the operation count for updating the flow field rises as the square of the number of vortices. When the number of the vortex particles is very large, the computation may become prohibitive due to the amount of required computing time.

Several methods aiming to reduce the computational cost of the N-body problem have been put forward including the hierarchical codes by Appel, Barnes and Hut[5,6], the algorithms based on multipole expansions by Greengard and Rokhlin [7,8], Van Dommelen and Rundensteiner [9] . But both methods are restricted to potential or singular type kernels. More recently , C. Draghicescu and M. Draghicescu developed a more general approach[10], in which high accuracy is achieved by high order Taylor expansions for both singular and smooth kernels. It also has the advantage of being mathematically simpler than multipole methods in 3-D cases. All these methods metioned above employ a hierarchical structure(N-body treecodes) and group the vortices spatially, then approximate the effects induced by each group at larger distance. Savings in computational cost result when the number of terms needed for multipole expansion or Taylor expansions is sufficiently small compared to the number of vortices in the group. They have the complexity of O(N) or O(NlogN) rather than $O(N^2)$ and work well in 2-D problems[7,9,10]. In 3-D, there is still a lack of systematical numerical tests for these algorithms [11,12].

In this report, the 3-D vortex particle method developed by Winckelmans and Leonard is reviewed and the numerical results are given for the fusion of two vortex rings . Some details for the implementation of the fast algorithm based on the Taylor expansions for the 3-D particle method are also discussed.

2. Governing Equations

The motion of incompressible viscous flow in 3-D can be described by the following equations

$$\frac{D\bar{\omega}}{Dt} = (\bar{\omega}\cdot\nabla)\bar{U} + \nu\nabla^2\bar{\omega} \tag{1}$$

$$\nabla\cdot\bar{U} = 0 \tag{2}$$

$$\bar{\omega} = \nabla\times\bar{U} \tag{3}$$

where $\bar{U}$ and $\bar{\omega}$ are the velocity and vorticity vectors respectively.

By using the concept of vector potential $\bar{\Psi}$ with $\bar{U} = \nabla\times\bar{\Psi}$ and assuming that $\bar{\Psi}$ itself is divergence-free, equation (3) can be written as

$$\nabla^2\bar{\Psi} = -\bar{\omega} \tag{4}$$

The equation of continuity(eq.(2)) is automatically satified by the introduction of the vector potential. The solution of eq.(4) is given by

$$\bar{\Psi}(X,t) = \int G(X-X')\bar{\omega}(X')dX' \tag{5}$$

where X' is the position of the volume element dX' and $G(X) = 1/(4\pi r)$ is the Green function of the Poisson equation in 3-D with $r = |X|$.

The velocity $\bar{U}$ can be obtained from the definition of $\bar{\Psi}$,

$$\bar{U} = \nabla\times\bar{\Psi} = \int K(X-X')\times\bar{\omega}(X')dX' \tag{6}$$

where $K(X) = -\frac{1}{4\pi}\frac{X}{r^3}$. Equation (6) is also called Biot-Savart law. Equation (1) and (6) determine the evolution of velocity and vorticity fields provided that an initial distribution of vorticity $\bar{\omega}(X,0)$ is given.

3. 3-D Vortex Particle Method

3.1 Regularized Vortex Particle Method

Vortex particles, also called vortex sticks or vortons, are an alternative to the vortex filaments. A position vector and a strength vector (=vorticity × volume) is associated to

each element which can be thought of as a small section of a vortex tube(circulation × length).

In the regularized version of the vortex particle method,the particle representation of the vorticity field is taken as

$$\begin{aligned}\tilde{\omega}_\sigma(X,t) &= \sum_p \overline{\omega}^p(t)\mathrm{vol}^p\zeta_\sigma(X-X^p(t)) \\ &= \sum_p \overline{\alpha}^p(t)\zeta_\sigma(X-X^p(t))\end{aligned} \tag{7}$$

where ζ_σ is a regularization function which is usually taken as radially symmetric and σ is smoothing radius (a cutoff length or core size) i.e.

$$\zeta_\sigma = \frac{1}{\sigma^3}\zeta(\frac{|X|}{\sigma}) \tag{8}$$

with the normalization

$$4\pi\int_0^\infty \zeta(\rho)\rho^2 d\rho = 1 \tag{9}$$

The velocity field induced by $\tilde{\omega}_\sigma(X,t)$ is computed from Biot-Savart law

$$\overline{U}_\sigma(X,t) = -\frac{1}{4\pi}\sum_p \frac{(X-X^p(t))}{|X-X^p(t)|^3} q(|X-X^p(t)|/\sigma)\times\overline{\alpha}^p(t) \tag{10}$$

where $q(\rho) = \int_0^\rho \zeta(t)t^2 dt$.

The evolution equations for the particle position and strength vector are

$$\frac{d}{dt}X^p(t) = \overline{U}_\sigma(X^p(t),t) \tag{11}$$

$$\frac{d}{dt}\overline{\alpha}^p(t) = (\overline{\alpha}^p(t)\cdot\nabla)\overline{U}_\sigma(X^p(t),t) \quad \text{(classical scheme)} \tag{12}$$

$$\frac{d}{dt}\overline{\alpha}^p(t) = (\overline{\alpha}^p(t)\cdot\nabla^T)\overline{U}_\sigma(X^p(t),t) \quad \text{(transpose scheme)} \tag{13}$$

$$\frac{d}{dt}\overline{\alpha}^p(t) = \frac{1}{2}(\overline{\alpha}^p(t)\cdot(\nabla+\nabla^T)\overline{U}_\sigma(X^p(t),t) \quad \text{(mixed scheme)} \tag{14}$$

According to the analysis by Winckelmans only the transpose scheme leads to the exact conservation of the total vorticity and a weak solution of equation (13). So only the eq.(11) and (13) are used for the following computations.

The effects of viscous diffusion can be considered by the use of an integral representation for the Laplacian operator $\nabla^2\overline{\omega}$. In this method,the following term is added to the right-hand side of (12)-(14):

$$\frac{2\nu}{\sigma^2}\sum_q(\mathrm{vol}^p\overline{\alpha}^q(t)-\mathrm{vol}^q\overline{\alpha}^p(t))\eta_\sigma(X^p(t)-X^q(t)) \tag{15}$$

where $\eta_\sigma(X)=\eta(|X|/\sigma)/\sigma^3$ and $\eta(\rho)=-\frac{1}{\rho}\frac{d}{d\rho}\zeta(\rho)$.

By using the high order algebraic smoothing $\zeta(\rho)=\frac{15}{8\pi}\frac{1}{(\rho^2+1)^{7/2}}$, the final expressions for the evolution of a set of vortex particles are

$$\frac{d}{dt}X^p=-\frac{1}{4\pi}\sum_q\frac{(|X^p-X^q|^2+2.5\sigma^2)}{(|X^p-X^q|^2+\sigma^2)^{5/2}}(X^p-X^q)\times\alpha^q \tag{16}$$

$$\begin{aligned}\frac{d}{dt}\alpha^p=\frac{1}{4\pi}\sum_q\Big[&-\frac{(|X^p-X^q|^2+2.5\sigma^2)}{(|X^p-X^q|^2+\sigma^2)^{5/2}}\alpha^p\times\alpha^q\\&+3\frac{(|X^p-X^q|^2+3.5\sigma^2)}{(|X^p-X^q|^2+\sigma^2)^{7/2}}(\alpha^p\cdot((X^p-X^q)\times\alpha^p))(X^p-X^q)\\&+105\nu\frac{\sigma^4}{(|X^p-X^q|^2+\sigma^2)^{9/2}}(\mathrm{vol}^p\alpha^q-\mathrm{vol}^q\alpha^p)\Big]\end{aligned} \tag{17}$$

From the viewpoint of physics, the viscous diffusion in fluid results from the random interaction of molecules and the non-uniformity of the fluid motion. The molecular interactions extend over a small distance , so the quantity of the viscous diffusion at a point is determined only by the fluid in the neighbourhood of that point. In the discrete particle method, it can be shown from eq. (17) that for any point X^p only the nearby particles have the most contributions to its viscous term because the function $\sigma^4/(|X^p-X^q|^2+\sigma^2)^{9/2}$ decays very fast (by the order of $1/|X|^9$) as the distance $|X^p-X^q|$ increases. So when the viscous term at a point X^p is calculated the summation is only applied to those particles X^q which satisfy $|X^p-X^q|\le 5\sigma$. Thus, some reductions in the computational cost can be achieved.

3.2 Relaxation of the Particle Vorticity Divergence

The vorticity field constructed by eq.(7) is not generally divergence-free:

$$\nabla\cdot(\tilde{\omega}_\sigma(X,t))=\sum_p \nabla(\zeta_\sigma(X-X^p(t)))\cdot\bar{\alpha}^p(t) \tag{18}$$

The divergence-free vorticity field $\omega_\sigma(X,t)$ can be reconstructed by taking the curl of the velocity field (eq. (10)). The procedure is as follows: if and when $\tilde{\omega}_\sigma(X,t)$ becomes a poor representation of the divergence-free field $\omega_\sigma(X,t)$,assign new particle strength $\bar{\alpha}^p_{new}(t)$ by imposing that $\tilde{\omega}_\sigma(X(t),t)=\omega_\sigma(X(t),t)$, which leads to solve the system of linear equations for all particles p:

$$\sum_q \bar{\alpha}^q_{new}(t)\zeta_\sigma(X^p(t)-X^q(t))=\nabla\times\bar{U}_\sigma(X^p(t),t) \tag{19}$$

4. Fast Algorithm

In this report , the fast algorithm based on Taylor expansions is extended to 3-D particle method. The basic ideas and 2-D examples are given in [10]. As shown in eq.(16), the smooth kernel for evaluating velocity field $\bar{U}_\sigma(X,t)$ has the form

$$K_\sigma(X,Y)=\frac{|X-Y|^2+2.5\sigma^2}{(|X-Y|^2+\sigma^2)^{5/2}}(X-Y). \tag{20}$$

It is difficult to use this expression into the fast algorithms available. The purpose of introduction of core size σ is to avoid the infinite self-induced velocity in the singular kernel. But as |X-Y| becomes large, the smooth kernel will be equivalent to singular kernel $K(X,Y)=(X-Y)/|X-Y|^3$. So only the singular kernel is considered in the following fast summation agorithm.

4.1 Mesh Structure

Assume that φ is an $a\times b\times c$ rectangular parallelepiped with $a\le b\le c$. We will cover φ with a hierarchy of 3-D meshes with rectangular boxes defined below. The set σ of all boxes is $\sigma=\sigma_0\cup\sigma_1\cup...\cup\sigma_H$, where σ_k is the set of boxes of level k defined recursively as follows: k=0: $\sigma_0=\{\varphi\}$.

$k\ge1$: The boxes in σ_k are obtained by cut a box in σ_{k-1}into two equal rectangular parallelepiped(the longest is split in half).

In σ_k there are 2^k cells of volume $2^{-k}(a\times b\times c)$ and the total number of boxes is $2^{H+1}-1$,forming a complete binary tree of height H with φ at the root.

We will denote by τ an arbitrary box with center Y_τ and radius $\rho(\tau)=\sup\{|Y-Y_\tau|:Y\in\tau\}$.

For each point X, we will partition φ into a collection $\Im(X)$ of boxes(at different levels) as follows:

1. Set $\Im(X)=\varnothing$ and $\tau=\varphi$.
2. If τ is empty or τ contains only X or $\tau\in\sigma_H$ then exit.
3. else if $d(X,\tau)\geq M\rho(\tau)$ then add τ to $\Im(X)$, where M is a given constant larger than one
4. else split τ into its two children and apply steps 2-4 recursively to the children.

4.2 Taylor Expansion

Fix point X and $\tau\in\Im(X)$, we will approximate the kernel $K(X,Y)=(X-Y)/|X-Y|^3$, $Y\in\tau$, by its Taylor polynomial of degree $\lambda-1$. The 3-D Taylor expansion of degree $\lambda-1$ of $f(X,Y)=1/|X-Y|^3$ with respect to Y about Y_τ is

$$f(X,Y)=P_{\lambda-1}(X,Y,Y_\tau)+R_{\lambda-1}(X,Y,Y_\tau) \tag{21}$$

$$\text{where } P_{\lambda-1}(X,Y,Y_\tau)=\sum_{|K|\leq\lambda-1}\frac{1}{K!}D_Y^K f(X,Y)_{Y=Y_\tau}(Y-Y\tau)^K$$
$$=\sum_{|K|\leq\lambda-1}a_K(X,Y_\tau)(Y-Y_\tau)^K, \tag{22}$$

and $K=(K_1,K_2,K_3), |K|=K_1+K_2+K_3, K!=K_1!K_2!K_3!, D_Y^K=\partial^{|K|}/\partial Y_1^{k_1}\partial Y_2^{k_2}\partial Y_3^{k_3}$, $Y^k=Y_1^{k_1}Y_2^{k_2}Y_3^{k_3}$.

The coefficients $a_K(X,Y_\tau)=\frac{1}{K!}D_Y^K f(X,Y)_{Y=Y_\tau}$ can be computed using the recurrence which is given in Appendix A. From the recurrence, it can be shown that the remainder $|R_{\lambda-1}|$ has the order $O(\frac{|Y-Y_\tau|^\lambda}{|X-Y_\tau|^{\lambda+3}})$ and the relative error $|R_{\lambda-1}|$ $/f(X,Y_\tau)$ has the order $O(\frac{|Y-Y_\tau|^\lambda}{|X-Y_\tau|^\lambda})$, or $O((\frac{\rho}{d})^\lambda)$. If $d\geq M\rho, (\frac{\rho}{d})^\lambda\to 0$ as $\lambda\to\infty$. So for a given small number ε, we can choose λ to be the smallest positive integer such that the relative error $|R_{\lambda-1}|/f(X,Y_\tau)\sim\varepsilon$.

Let $K^{\lambda,\tau}(X,Y)=P_{\lambda-1}(X,Y,Y_\tau)$, we will now define the approximation to $\overline{U}_\sigma(X,t)$ (time t will be fixed and omitted) as

$$\tilde{U}(X)=\sum_{\tau\in\Im(X)}\tilde{U}^\tau(X)+\text{ direct summation term(near field)} \tag{23}$$

The expression for $\tilde{U}^\tau(X)$ can be found in Appendix B.

The evaluation of $\tilde{U}(X)$ reduces to the following three steps:

1. preprocessing: evaluate the sums(eq.(26)) for all cells τ and indices K;

2.for all cells $\tau \in \Im(X)$ compute $\tilde{U}^{\tau}(X)$ according to eq.(25) and then add them together.

3.computing the direct summation term in eq(23) using the smooth kernel.

In 3-D computations, because of the existence of the stretching term in the vorticity transport equation,the derivative of the velocity is also required. This can be obtained from the derivative of the right-hand term in eq.(25).

5. Numerical Results

To demonstrate its ability to calculate unsteady viscous flows, the 3-D vortex particle method is applied to the calculation of the interaction of two vortex rings. The initial conditions (Fig.1) for the computation are as follows

$\Gamma = 1$, (circulation of each vortex ring)

$R = 1$, (radius of each vortex ring)

$S = 2.7$, (distance between centers of two vortex rings)

$\theta_0 = 15^{\circ}$, (the angle between the plane of vortex rings and horizontal plane)

$Re = \Gamma / \nu = 400$, (the Reynolds number based on circulation Γ)

$\omega_{\varphi} = \frac{\Gamma}{2\pi a} e^{-r^2/2a^2}$, (initial vorticity distribution within the core of the vortex ring, a=0.1 and r is measured from the center of the core).

The mesh is constructed using N_{φ} cross sections of torus separated by an angle $\Delta\varphi = 2\pi / N_{\varphi}$ and N_s cells within each cross section (Fig. 2). The elements within each cross section of the ring are arranged on n_c radial locations and each cell has an equal area πr_l^2. The center of each vortex element is located at its centroid X_i and the initial strength vector of vortex element is set equal to $\overline{\omega}(X_i, 0)dv_i$,where dv_i is the volume of each vortex element.

In the present computations, r_l=0.05, n_c=3, N_s=49, N_{φ}=64, so the total number of the vortex particles used is 6272. The core size of each element σ=0.065 . The Adams-Bashforth second order method is employed for the integration of eq.(11) and (13) and the time step is 0.01.

Fig.3 gives nine snapshots of the calculated result which shows the interaction and

fusion process of two vortex rings. At first the two vortex rings approach gradually and then collide with each other . As time elapses ,they eventually fuse into another single vortex ring.

In the computation , no particle addition or relaxation of $\nabla \cdot \tilde{\omega}_\sigma$ is used. The CPU time used for T=8 is about 72 hours on the SGI workstation.

6. Conclusions and Remarks on Future Works

In this report, the 3-D vortex particle method is applied to the computation of unsteady viscous flow. An example is given for the fusion of two vortex rings, which shows that this method works well for long time calculations even though there is no particle addition and no relaxation of divergence of vorticity . Due to the high computational cost of the method, some fast algorithms and the parallel computations are needed for long time calculations and for large number of vortex particles.

The ultimate goal of the study is to develop a 3-D code which takes advanage of the discrete vortex particle method and is suitable for the simulation of unsteady incompressible viscous flows around the finite wings in the condition of dynamic stall. Many complicated physical phenomena such as 3-D seperation flows and unsteady effects etc. are associated with the problem. The importance of the study is obvious in both theoretical and practical aspects. The difference between unbounded flow and the flow past a body lies in the fact that the vorticity will generate at the body surface in order to satisfy the no-slip condition. To apply the 3-D discrete vortex particle method,the surface of the wing should be discretized into a set of planar quadrilateral panels. The boundary condition is satisfied at the center of each panel and the new vortex particles will generate there. The velocity at a point can be determined by the contributions from the free stream, vortex particles around the wing and the boundary conditions at the wall. To construct an accurate, efficient and robust 3-D discrete vortex code, the following aspects will be taken into considerations:

(1) Study of the discrete vortex methods which satisfy (or essentially satisfy) the condition of divergence-free of the vorticity field.

(2) Parallel implementation of the code and the fast algorithm.

(3) The mechanism of the vortex creation at the wall.

(4) The conservation laws for some flow quantities in 3-D.

Reference

1. Spalart P R , NASA TM 100068, June 1988
2. Winckelmans G S, Leonard A, J. Comput. Phys. **109,** 247-273, 1993.
3. Batchelor G R , An Introduction to Fluid Dynamics, 1967 . (Cambridge University Press)
4. Leonard A, Annu. Rev. Fluid Mech. **17** ,523,1985.
5. Appel A W,SIAM J. Sci.Stat.Comput. **6** ,85-103,1985.
6. Barnes J and Hut P , Nature **324** ,446,1986.
7. Greengard L and Rokhlin, J. Comput. Phys. **73**,325,1987
8. Greengard L and Rokhlin, in Lecture Notes in Mathematics, Vol.1360,121,1988.
9. van Dommelen L and Rundensteiner E A , J. Comput. Phys. **83** ,126,1989.
10. Draghicescu C I and Draghicescu M ,J. Comput. Phys. **116,**69,1995.
11. Schmidt K E and Lee M A ,J. Statistical Physics, Vol.63 ,1223,1991.
12. Pringle G J ,PhD thesis, Napier University, Edinburgh,1994.

Appendix A The Recurrence Relations for the Coefficients

$$a_K(X,Y_\tau)=\frac{1}{K!}D_Y^K f(X,Y)_{Y=Y_\tau}$$

$$a_{0,0,0}=f(X,Y_\tau), \tag{24a}$$

$$\begin{aligned}a_{K_1,K_2,K_3}=g^2[&\frac{2K_1+1}{K_1}(X_1-Y_{\tau1})a_{K_1-1,K_2,K_3}+2(X_2-Y_{\tau2})a_{K_1,K_2-1,K_3}\\&+2(X_3-Y_{\tau3})a_{K_1,K_2,K_3-1}-\frac{K_1+1}{K_1}a_{K_1-2,K_2,K_3}\\&-a_{K_1,K_2-2,K_3}-a_{K_1,K_2,K_3-2}],\quad K_1\neq 0,\end{aligned} \tag{24b}$$

$$\begin{aligned}a_{K_1,K_2,K_3}=g^2[&2(X_1-Y_{\tau1})a_{K_1-1,K_2,K_3}+\frac{2K_2+1}{K_2}(X_2-Y_{\tau2})a_{K_1,K_2-1,K_3}\\&+2(X_3-Y_{\tau3})a_{K_1,K_2,K_3-1}-a_{K_1-2,K_2,K_3}\\&-\frac{K_2+1}{K_2}a_{K_1,K_2-2,K_3}-a_{K_1,K_2,K_3-2}],K_2\neq 0,\end{aligned} \tag{24c}$$

$$\begin{aligned}a_{K_1,K_2,K_3}=g^2[&2(X_1-Y_{\tau1})a_{K_1-1,K_2,K_3}+2(X_2-Y_{\tau2})a_{K_1,K_2-1,K_3}\\&+\frac{2K_3+1}{K_3}(X_3-Y_{\tau3})a_{K_1,K_2,K_3-1}-a_{K_1-2,K_2,K_3}\\&-a_{K_1,K_2-2,K_3}-\frac{K_3+1}{K_3}a_{K_1,K_2,K_3-2}],K_3\neq 0,\end{aligned} \tag{24d}$$

where $g^2 = \dfrac{1}{(X_1 - Y_{\tau 1})^2 + (X_2 - Y_{\tau 2})^2 + (X_3 - Y_{\tau 3})^2}$; $a_{i,j,k} = 0$ if i<0 or j<0,or k<0.

Appendix B The Expression For $\tilde{U}^{\tau}(X)$

$$\begin{aligned}
\tilde{U}^{\tau}(X) &= -\frac{1}{4\pi}\sum_{Y_j \in \tau} K^{\lambda,\tau}(X, Y_j)(X - Y_j) \times \alpha_j \\
&= -\frac{1}{4\pi}\sum_{Y_j \in \tau}[(X_2 - Y_{j2})\alpha_{j3} - (X_3 - Y_{j3})\alpha_{j2}, \\
&\qquad (X_3 - Y_{j3})\alpha_{j1} - (X_1 - Y_{j1})\alpha_{j3}, \\
&\qquad (X_1 - Y_{j1})\alpha_{j2} - (X_2 - Y_{j2})\alpha_{j1}] \sum_{|K| \le \lambda - 1} a_K(X, Y_\tau)(Y_j - Y_\tau)^K \\
&= -\frac{1}{4\pi}\sum_{|K| \le \lambda - 1} a_K(X, Y_\tau)[(X_2 A_\tau^K - B_\tau^K - X_3 C_\tau^K + D_\tau^K), \\
&\qquad (X_3 E_\tau^K - F_\tau^K - X_1 A_\tau^K + G_\tau^K), \\
&\qquad (X_1 C_\tau^K - H_\tau^K - X_2 E_\tau^K + I_\tau^K)]. \qquad (25)
\end{aligned}$$

and

$$\begin{aligned}
&A_\tau^K = \sum_{Y_j \in \tau} \alpha_{j3}(Y_j - Y_\tau)^K, B_\tau^K = \sum_{Y_j \in \tau} Y_{j2}\alpha_{j3}(Y_j - Y_\tau)^K, \\
&C_\tau^K = \sum_{Y_j \in \tau} \alpha_{j2}(Y_j - Y_\tau)^K, D_\tau^K = \sum_{Y_j \in \tau} Y_{j3}\alpha_{j2}(Y_j - Y_\tau)^K, \\
&E_\tau^K = \sum_{Y_j \in \tau} \alpha_{j1}(Y_j - Y_\tau)^K, F_\tau^K = \sum_{Y_j \in \tau} Y_{j3}\alpha_{j1}(Y_j - Y_\tau)^K, \\
&G_\tau^K = \sum_{Y_j \in \tau} Y_{j1}\alpha_{j3}(Y_j - Y_\tau)^K, H_\tau^K = \sum_{Y_j \in \tau} Y_{j1}\alpha_{j2}(Y_j - Y_\tau)^K, \\
&I_\tau^K = \sum_{Y_j \in \tau} Y_{j2}\alpha_{j1}(Y_j - Y_\tau)^K. \qquad (26)
\end{aligned}$$

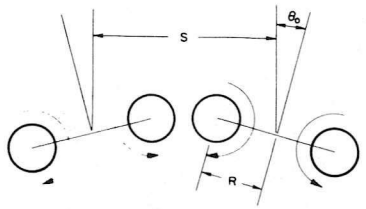

FIG. 1. Initial condition for the computation of the collision of two vortex rings.

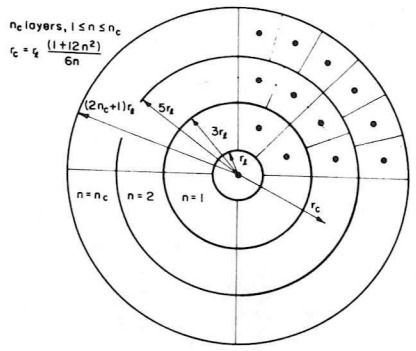

FIG. 2. Discretization of the core of a vortex tube. Each cell has an equal area πr_f^2.

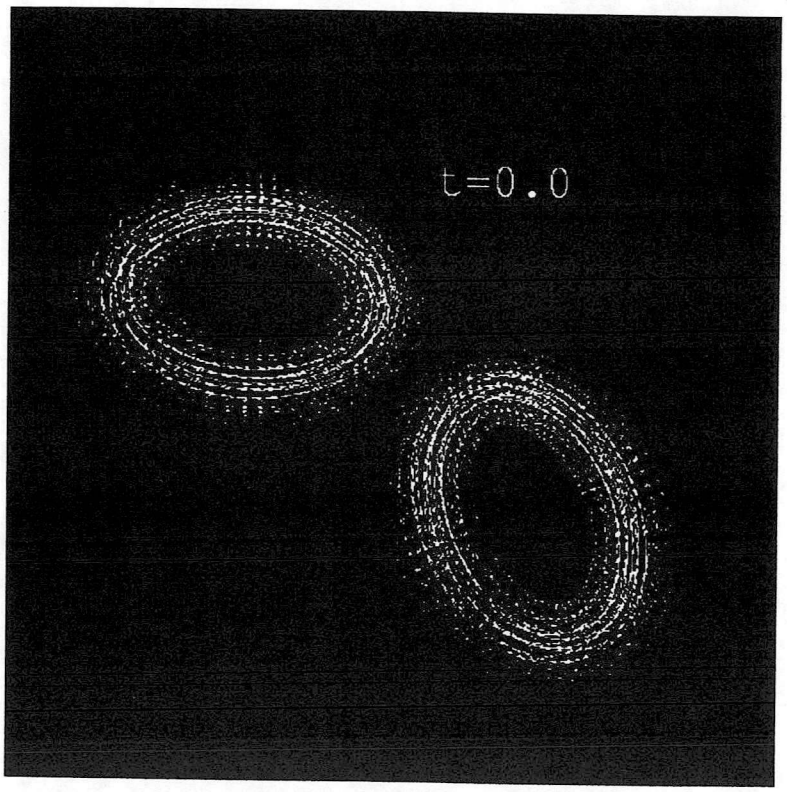

Fig.3 Fusion of two vortex rings using DVP method (view of strength vector)

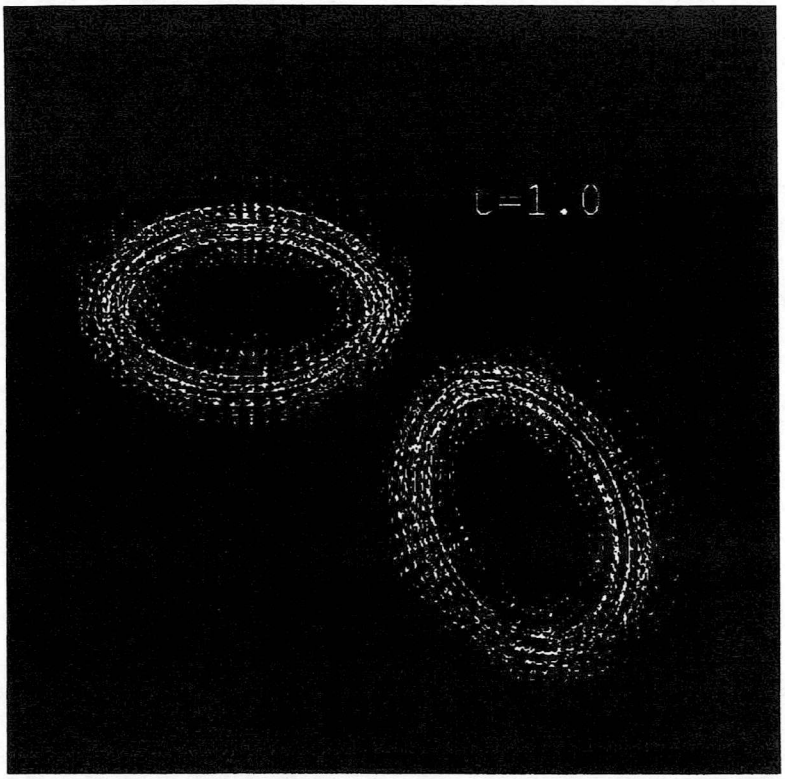

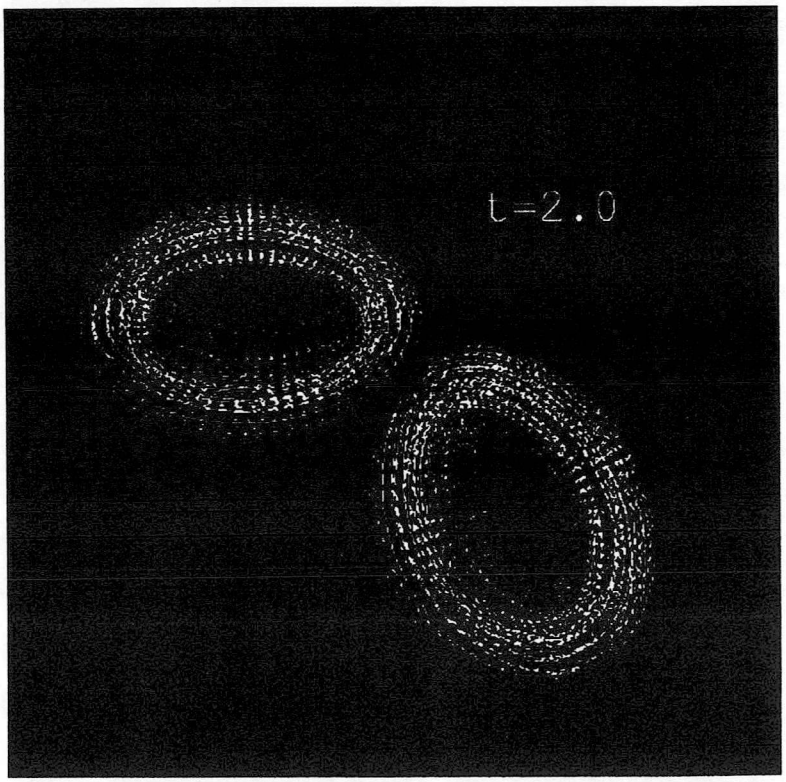

Fig.3 (continued)

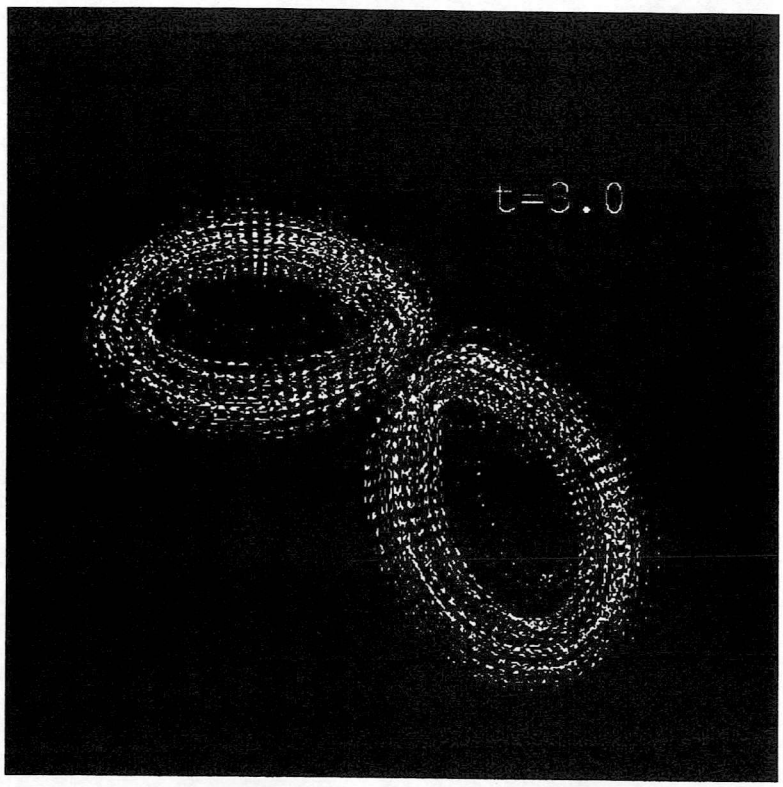

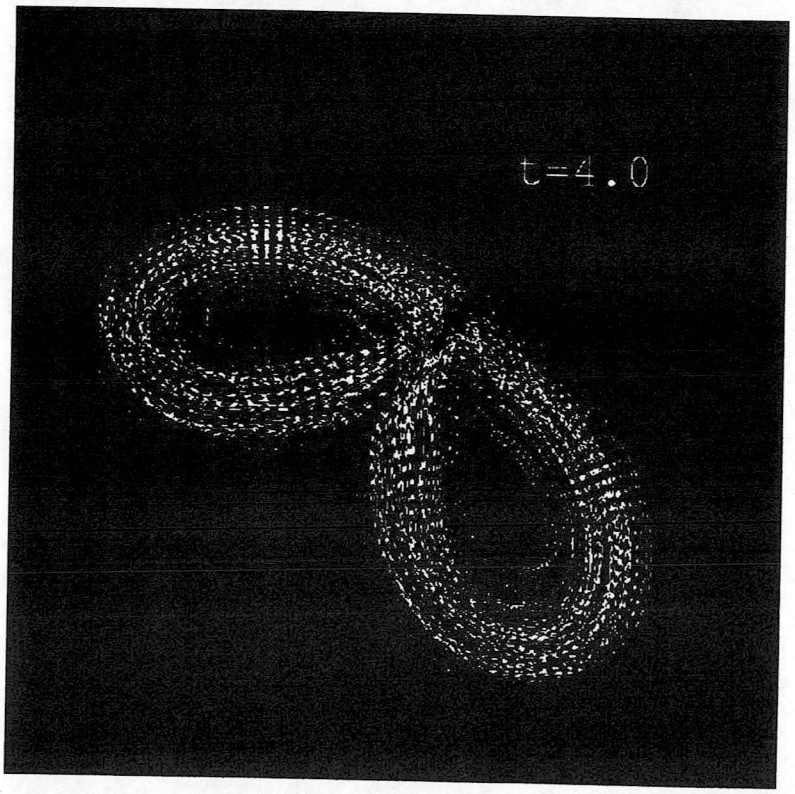

Fig.3 (continued)

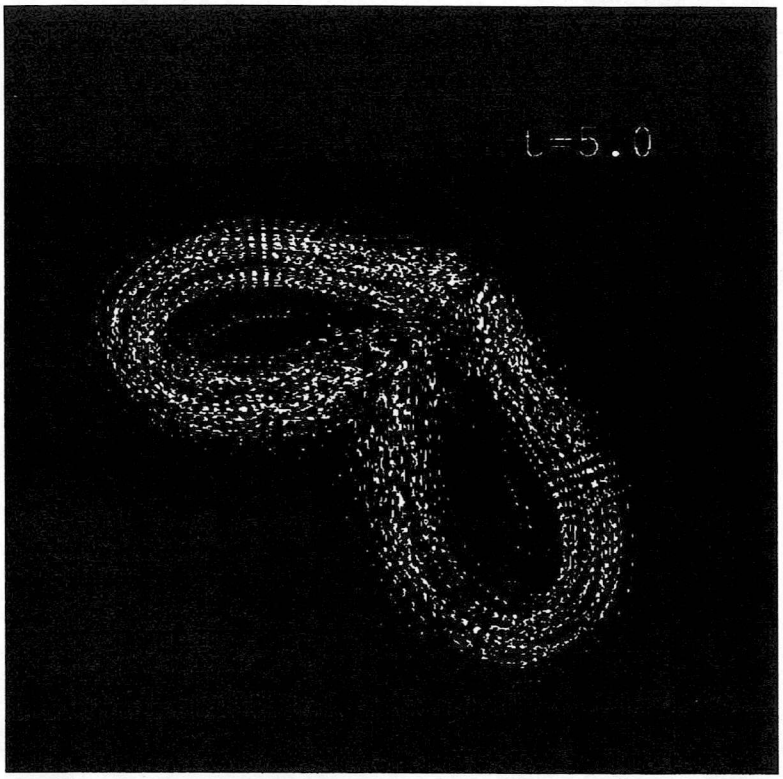

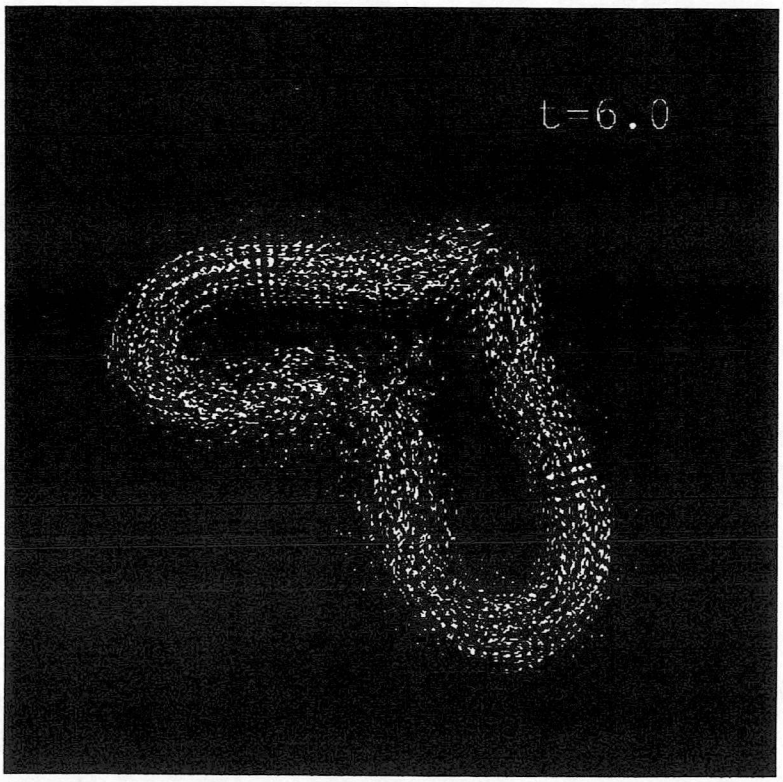

Fig.3 (continued)

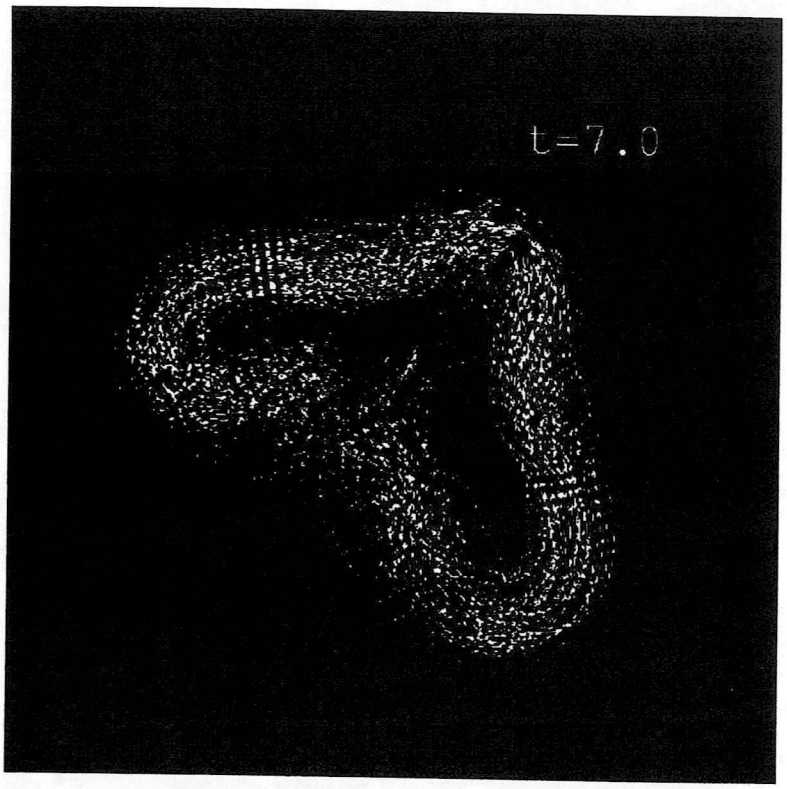

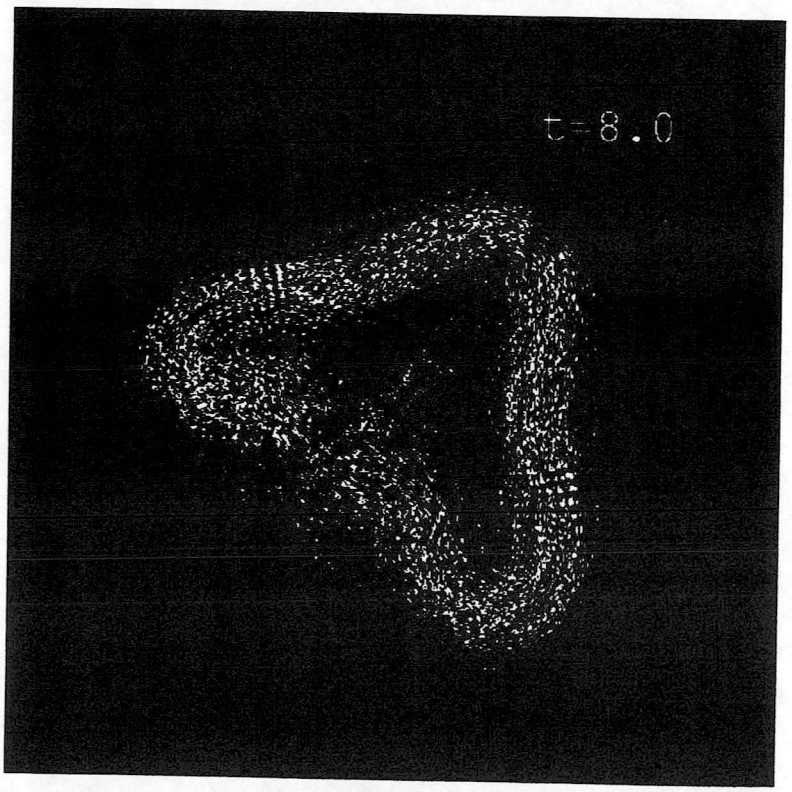

Fig.3 (continued)